Chapter 7

NEUTRON ANALYSIS

As mentioned in chapter 4, the MuSun experiment includes a set of eight auxiliary neutron detectors in addition to the primary electron detector array. Although decay electrons are easier to detect and permit a more precise extraction of the muon capture rate, direct detection of neutrons remains a valuable tool. The primary challenge in accurately measuring the capture rate from the neutron signal lies in the exact determination of the detection efficiency. This concern becomes much less important when it comes to studies of the relative signal strength from different locations in time or space. The neutron signals are also more sensitive to details of the muon's interactions, making them ideal for several systematics studies.

One area where the neutron detectors are useful is in monitoring the muon kinetics in deuterium. The MuSun experiment aims to specifically measure the capture rate from the doublet state, so accurate measurement and modeling of the kinetics is very important. Because the capture rates from both hyperfine states are much smaller than the muon decay rate, the total lifetime as well as the electron signal are largely insensitive to this effect. In contrast, the neutron signals are sensitive to the hyperfine state, and the resulting time dependence is plainly visible in the data.

Another place the neutron detectors have an advantage is in studying wall stops. Consider an extremely simple kinetics model which only includes a single bound state from which muons may either decay or undergo nuclear capture. The rates of electron and neutron

production as a function of time are then

$$R_e(t) = N_0 \lambda e^{-(\lambda+\Lambda)t} \tag{7.1}$$

$$R_n(t) = N_0 y_n \Lambda e^{-(\lambda+\Lambda)t} \tag{7.2}$$

where λ is the muon decay rate, Λ is the capture rate, N_0 is the total number of muons, and y_n is the average neutron yield from a muon capture reaction. The neutron yield is 2 for deuterium, but may take on different values depending on the stop material. The capture rate Λ is proportional to the fourth power of Z, and for the high Z materials used in the TPC typical values are on the order of 10 μs^{-1} or about 20 times greater than the decay rate. At such high capture rates, we expect a neutron signal comparable to the electron signal even when factoring in the lower detector efficiency. Furthermore, a small admixture of wall stops will stand out much more relative to the small signal from the good stops in deuterium.

7.1 Neutron Sources

We identify five dominant sources of neutrons, several of which are highlighted in figure 7.1:

7.1.1 Muon Capture in Deuterium

First, there are of course the neutrons produced by the nuclear muon capture reactions MuSun was designed to study. Because muon capture and muon decay both convert the muon into a neutrino, the two reactions are mutually exclusive. Thus, a muon capture event is characterized by the lack of any decay electron. However, the 70% solid angle coverage of the electron detectors limits the efficiency of an electron veto. With regard to the TPC, capture events have no special features and appear identical to normal decays. Muon capture on deuterium produces three output particles, yielding neutrons with a continuous energy distribution that peaks around 1.5 MeV but extends as high as 50 MeV. These events produce a pair of coincident neutrons which could in principle allow accurate tagging of capture events, but the efficiency of the MuSun neutron detectors is too low for this to be practical.

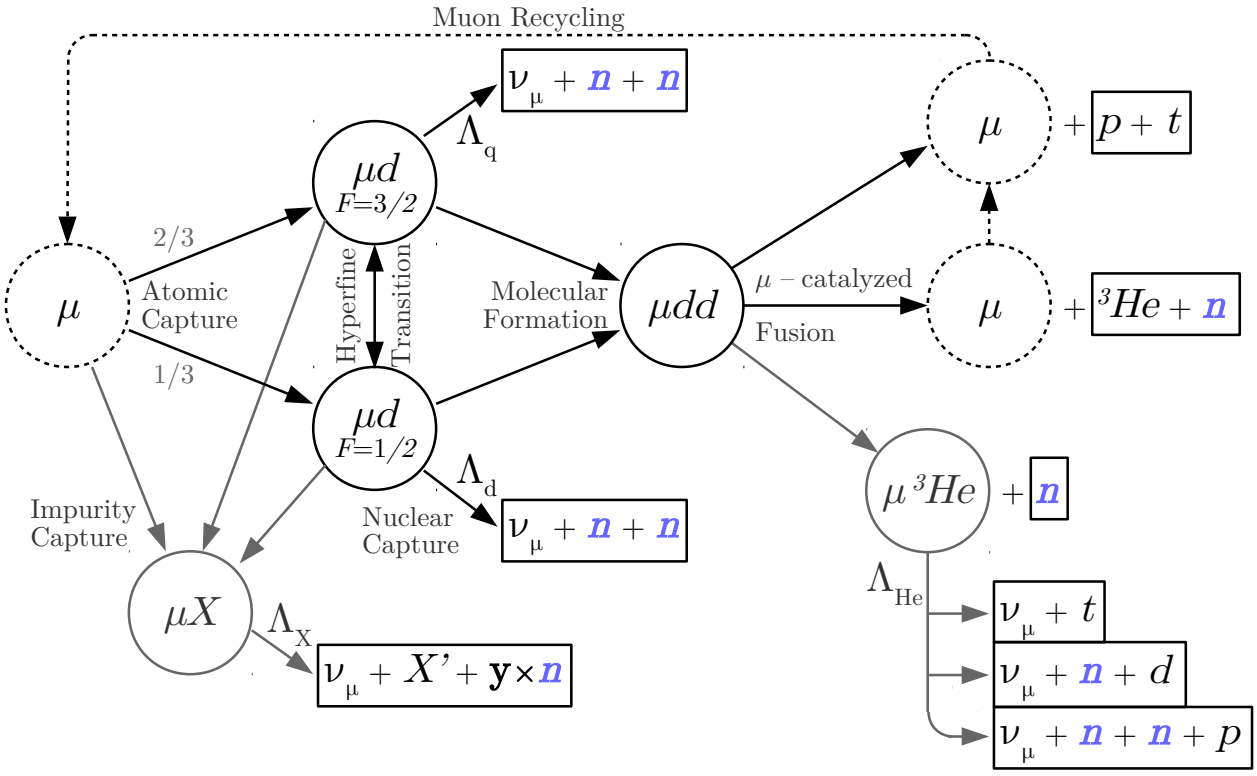

Figure 7.1: Full muon kinetics in D_2 gas. Neutron emissions are highlighted in blue.

Capture may occur in both of the hyperfine states, but at significantly different rates. For the doublet state, we expect a rate of approximately 400 s^{-1}, compared to only 10 s^{-1} for the quartet state. This difference in the capture rates produces a time distribution similar to the muon lifetime at late times, but with a buildup at early times as muons in the quartet state transition to the doublet state.

7.1.2 Muon Catalyzed Fusion

Muons in deuterium also undergo muon catalyzed fusion, and in the case of ^3He fusion a neutron is produced. Muon catalyzed fusion events are characterized by additional energy deposition in the TPC by fusion products. For p-t fusions this energy deposition is large, but ^3He deposits much less energy and the events are not cleanly separated from normal muon

stops. To improve our ability to distinguish these events a two dimensional cut is defined in E0-E1 space, as shown in figure 7.2.

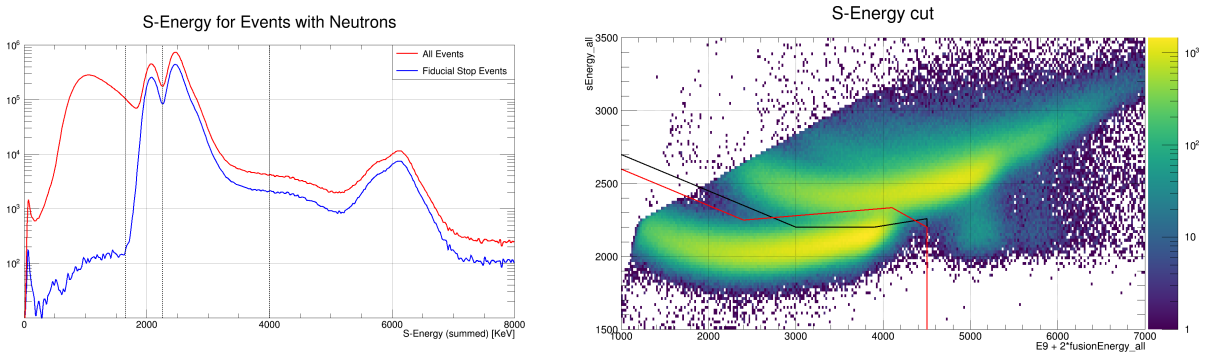

Figure 7.2: Two Dimensional cuts defined based on S- and T-Energy. The black line is defined based on the fusion distribution, while the red is defined based on the captures.

Muon catalyzed fusion is non-destructive, so most fusion events are accompanied by an electron from the subsequent decay of the muon. The sticking probability for ^3He fusions is 12%, and stuck muons may capture on the ^3He potentially producing one or two additional neutrons. The remaining 88% of ^3He fusions produce a free muon, which is recycled and has the possibility of catalyzing one or more additional fusion reactions before decaying. Multiple fusions and ^3He capture are both very rare events, and are currently neglected in the neutron analysis. Muon catalyzed fusion essentially has a two body final state, yielding mono-energetic neutrons at 2.45 MeV.

At the experimental temperature of 30K, the rate of muon catalyzed fusion is approximately 4,000,000 s^{-1} from the quartet state and 50,000 s^{-1} from the doublet state. The fusion time distribution therefore starts with a very large signal which rapidly decays as muons transition to the doublet state.

7.1.3 Muon Capture on Other Materials

Recall that the rate of nuclear muon capture is proportional to the fourth power of Z of the capturing material. Any muons which capture on other materials besides deuterium will

produce a large signal. There are two potential sources of such events in MuSun: impurities in the gas or muon stops in the walls.

Gas impurities were a major concern in the design of the MuSun experiment. In addition to muons which stop directly on impurities, muons on deuterium will transfer to higher-Z atoms in the case of a collision. This effect significantly amplifies the signal from even trace amounts of impurity. However, the CHUPS system keeps the impurity concentration controlled to the 1 ppb level, which should be enough to make the impurity signal negligible.

Alternatively, muons which stop in the container walls or TPC structure will also produce capture neutrons. The TPC is designed to ensure the muons stop in the gas well away from the walls, but tracking failures can allow some wall stops to masquerade as good fiducial volume stops. Like captures in deuterium, wall captures are characterized by a lack of an electron and a wide energy distribution extending at least to tens of MeVs. Wall captures are associated with somewhat reduced energy deposition in the TPC, as the muon does not fully come to a stop in the gas before hitting the wall and therefore the end of the Bragg peak is missing. The missing energy is generally too little to cleanly identify these events, although some very low energy events may be isolated as seen in figure 7.2. Finally, unlike other neutron sources wall stops should increase sharply with the proximity of the reconstructed stop position to any solid materials.

Wall stops will primarily come from the TPC structure, which is deliberately constructed of high-Z materials such as silver and tungsten. For these materials, capture rates are on the order of 10 μs^{-1} or about 20 times greater than the decay rate. Wall stop neutrons therefore produce a large signal which follows a fast exponential decay and quickly disappears.

7.1.4 Beam Background

In addition to neutrons produced by stops in the target, there are a large number of background neutrons. Some of these are due to constant background sources such as cosmic rays, but the majority are in the muon beam. The presence of neutrons in the beam is the result of muon capture from muons stopping in the beam pipe upstream of the target. These neutrons

have a low probability of being observed by the neutron detectors, but as the reactions all occur upstream of the MuSun entrance detectors there is no way to veto such events.

Because the beam background neutrons are essentially the result of wall stops, they share many characteristics with the wall stop neutrons. In particular they have similar energy spectra, although the beam pipe is made of iron so the exact distribution does not necessarily match the high-Z captures in the TPC walls. As the MuSun analysis requires a good muon entrance, these beam backgrounds can only appear in the data if they are coincident with another muon. Most beam background events are therefore characterized by a normal stop and subsequent decay electron, combined with an additional neutron.

All beam-related backgrounds in the MuSun experiment share a time-dependent background structure caused by the electrostatic kicker, refer to appendix A for a detailed description of the background structure.

7.1.5 Photo-Neutrons

Finally, the particles produced by muon capture or decay may undergo secondary reactions and produce additional neutrons. Most commonly, high energy gamma rays may be absorbed in the vessel walls and cause the emission of neutrons via photodisintegration. The properties of the resulting photo-neutrons closely match those of the gamma rays that produced them, which are discussed in the next section.

Despite the connection between the photo-neutrons and gamma rays, it is difficult to determine the proportionality factor between them. One reason is that photo-neutrons are not related to gamma rays of the same energy, but rather gamma rays with high energies potentially exceeding the dynamic range of the neutron detectors. In addition, the probability of a photodisintigration event depends on the amount of material the gamma ray passes through, which in turn depends on the muon stop position and gamma emission direction.

The photo-neutron signal is quite small and therefore difficult to measure directly, but it is an important correction when studying the deuterium capture neutron signal.

7.2 Gamma Sources

The MuSun neutron detectors are also sensitive to other particles besides neutrons. As the neutron detectors are positioned behind the eSCs, the majority of charged particles may be eliminated by a eSC coincidence veto. This still leaves gamma rays, which produce a large signal in the neutron detectors. These gamma signals have generally been treated as an uninteresting background, but they have proven interesting in recent analyses. We identify four classes of gamma signal.

7.2.1 Decay Electron Bremsstrahlung

First, a large number of gammas are produced as bremsstrahlung radiation caused by muon decay electrons. Similar to the photo-neutrons, bremsstrahlung gamma rays are produced by scattering in the detector structure and therefore depend on electron's path. This produces significant changes in the signal depending on the specifics of the muon stop and electron emission direction. Most notably, there is often a difference of more than a factor of two between the neutron detectors above the target and those below. The support structure below the TPC happens to be aligned with the lower neutron detectors, causing a large increase in observed scattering.

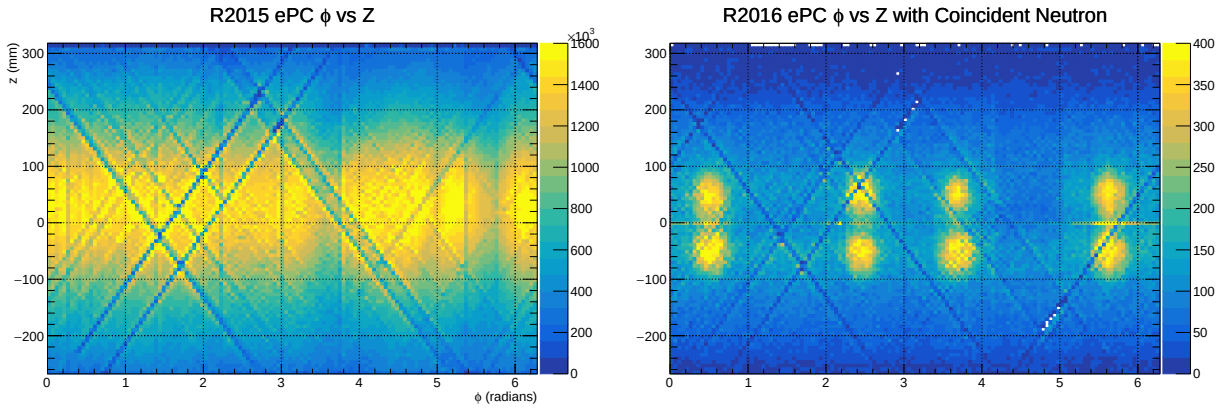

Figure 7.3: ePC ϕ vs Z for R2015 data (left) and R2016 data with neutrons selected (right).

The time dependence of these gamma rays matches the electron time distribution. In fact each bremsstrahlung photon should be coincident with the electron that emitted it. In practice though, many electrons are either absorbed or missed by the electron scintillators making coincidence cuts ineffective.

7.2.2 Nuclear Capture

Muon capture in deuterium splits the nucleus into a pair of unbound neutrons. In higher-Z materials though, muon capture leaves behind a daughter nucleus which is often in an excited state. The nucleus will then return to the ground state by emitting gamma rays. In principle these gamma rays should form distinct transition lines, but the complicated structure of high-Z nuclei produces a large number of lines which cannot be distinguished by the MuSun neutron detectors.

Because these gamma rays are emitted directly after muon capture, they follow the same time distribution as the wall capture neutron signal.

7.2.3 Atomic Capture

The most interesting feature of the gamma ray signals is the ability to observe gammas emitted during atomic capture. When muons are captured by an atom, they initially start at very high energy levels of n=20 or more. The muon then rapidly cascades down to the atomic ground state, emitting gammas with well-defined atomic transition energies in the process. This cascade process takes less than ten nanoseconds, producing a large gamma peak coincident with the muon entrance. Energy spectra for these prompt gammas from various target materials were observed in the 2016 calibration run, and are shown in figure 7.4.

The transition lines in deuterium have too little energy to be observable by the MuSun neutron detectors, but the $2 \rightarrow 1$ and $3 \rightarrow 2$ transitions are clearly visible for high-Z materials. The transition energies give us an additional way to identify the stop materials which is more accurate than estimating the capture rate. If the stop material distribution is

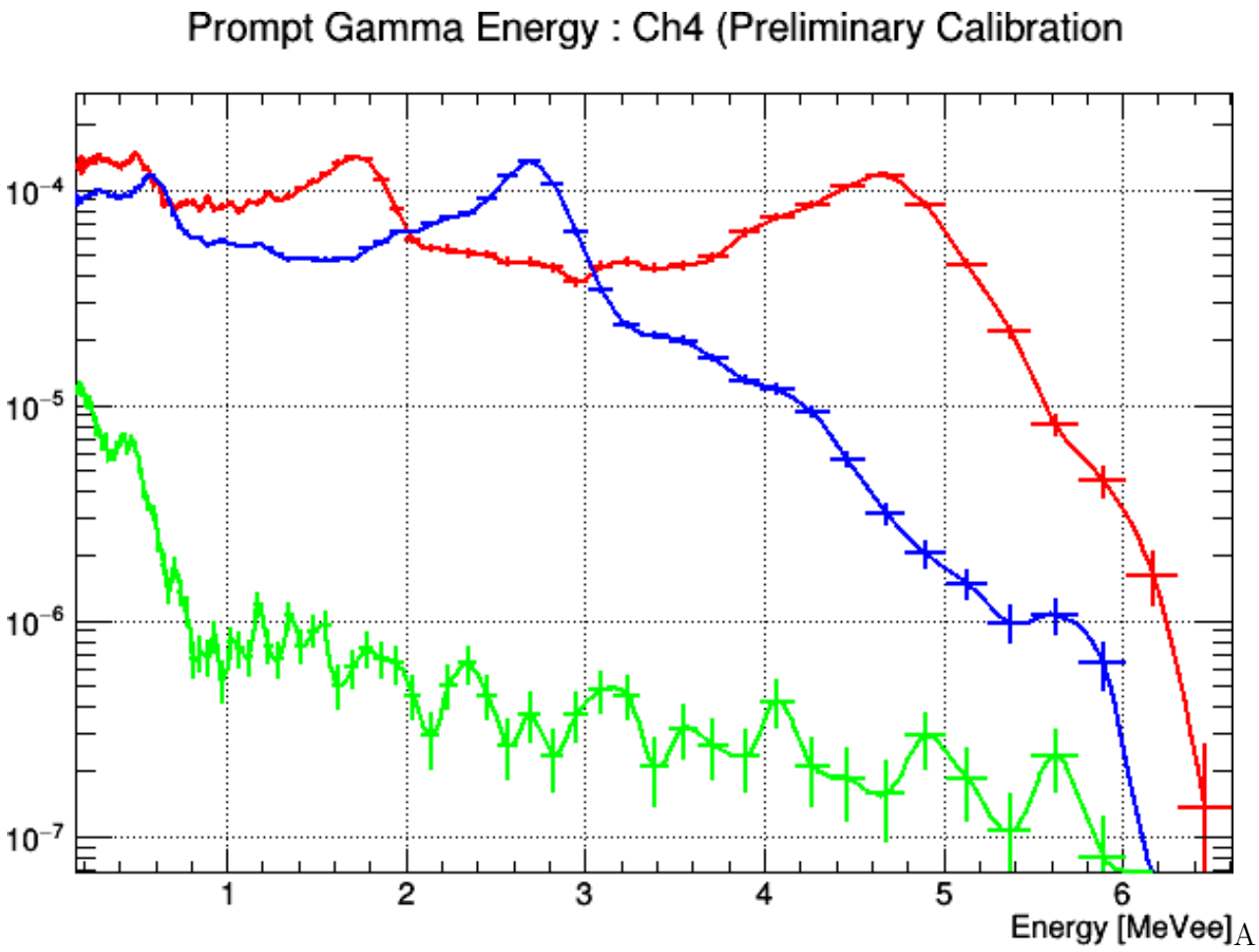

Figure 7.4: Atomic capture gamma energy spectra from R2016 calibration data.

well known, that can also be used to fix the capture rate used in the rest of the analysis. The atomic capture gamma pulse is also a distinctive signature of wall stops and can be detected with comparable sensitivity to the capture neutrons themselves.

The Macor signal is much smaller and lacks the clean high-energy peaks, but still emits some lower energy gammas which should be identifiable. Because the muon capture rate in macor is much lower than in the other TPC materials, stops in macor are very hard to detect by looking for capture neutrons. In this case, the atomic capture gammas may prove to be a much more useful signal for identifying such stops.

7.2.4 Beam Background

Finally, there is a large beam background gamma ray signal. This signal is mostly due to bremmstrahlung radiation from particles in the beam. The beam gamma background increases when the kicker is fired, since diverting the beam gives it more material to scatter on. Because the bremmstrahlung gammas are emitted without any delay, the gamma background exhibits the RF oscillation of the beam.

Table 7.1: Neutron detector signal summary

Particle	Signal	Electron	Energy	Source	Special Properties
Neutron	D Capture	none	smooth	D stops	two simultaneous neutrons
	^{3}He Fusion	delayed	peaked	D stops	additional TPC energy
	High-Z Capture	none	smooth	wall stops	
	Background	present	smooth	beam	
	Photo-Neutrons	prompt	smooth	scattering	
Gamma	Electron Brem.	prompt	smooth	scattering	
	Nuclear Capture	none	smooth	wall stops	
	Atomic Capture	none	peaked	wall stops	coincident with muon
	Background	present	smooth	beam	

7.3 Pulse Shape Discrimination

As mentioned in chapter 5, pulses caused by neutrons may be identified by their long tails following the initial peak. A pulse shape discrimination (PSD) cut is defined based on the fraction of the pulse area contained in the pulse tail. The pulse shapes change slightly with pulse energy so the PSD cut is also energy dependent, and plots of pulse tail fraction vs total area are referred to as PSD plots.

Now that the possible neutron and gamma signals are well understood, we can use that information to refine the PSD cuts and estimate their error rates. By selecting fusion events with a TPC energy cut or selecting stops near the walls to maximize high-Z captures, we may produce a distribution with a much higher proportion of neutrons than usual. Similarly, a distribution with predominantly gamma rays may be created by selecting events with a coincident muon entrance or electron. Figure 7.5 shows PSD plots with these cuts applied:

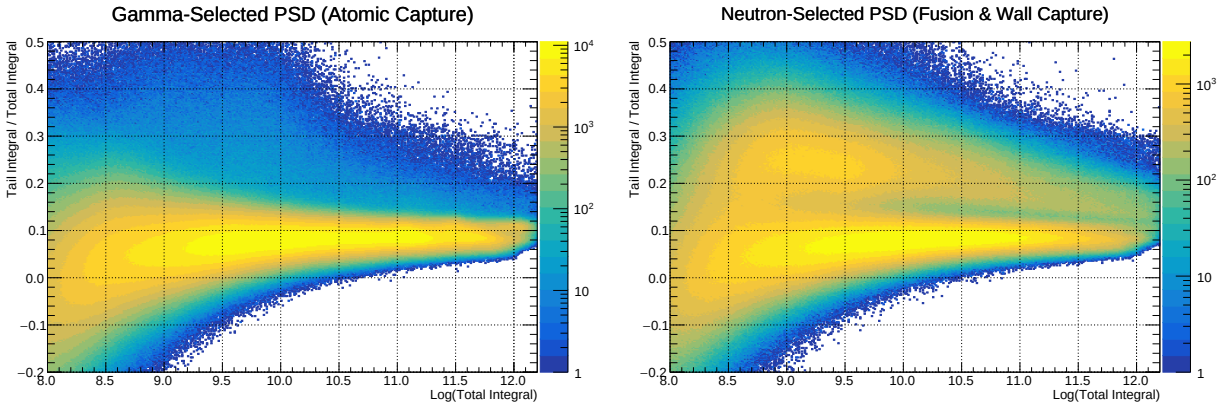

Figure 7.5: PSD plots with either atomic capture gammas (left) or wall stop and fusion neutrons selected (right)

For each energy slice, we attempt to separate these two distributions into pure neutron and gamma distributions. If F_1 and F_2 refer to the gamma and neutron selected events respectively, we can write them in terms of the true distributions F_γ and F_n:

$$F_1 = N_{1\gamma}F_\gamma + N_{1n}F_n \tag{7.3}$$

$$F_2 = N_{2\gamma}F_\gamma + N_{2n}F_n \tag{7.4}$$

where the N's are the numbers of each kind of event in either set. If we knew these values then extracting the true distributions would be a simple matter of scaling and subtracting

the two histograms:

$$F_\gamma = (F_1 N_{2n} - F_2 N_{1n})/(N_{1\gamma} N_{2n} - N_{2\gamma} N_{1n}) \tag{7.5}$$

$$F_n = (F_2 N_{1\gamma} - F_1 N_{2\gamma})/(N_{1\gamma} N_{2n} - N_{2\gamma} N_{1n}) \tag{7.6}$$

In practice, the proportion of neutrons and gammas in each set is unknown. Rough estimates may be obtained by fitting the neutron and gamma bands to a pair of gaussians, but overlap between the bands and any differences in their true shapes will produce errors with this method. More accurate values may be determined using the shape fitting method discussed in the next section.

Extraction of the true distributions is also somewhat problematic due to the statistical fluctuations of the data. The gamma-selected distribution is already quite pure, so subtracting a small proportion of neutrons has little effect. Neutrons cannot be selected with the same accuracy however, and the best neutron-selected distribution still has a majority of gamma events. Scaling and subtracting the gamma distribution therefore leaves large fluctuations in the place of the original gamma band. To mitigate this issue, the resulting distributions are smoothed before being analyzed further.

Finally, a PSD cut is defined based on the estimated pure distributions. Because the gamma signal is so large, our PSD cuts have been designed to suppress the gammas by various proportions. Figure 7.6 shows pure distributions extracted from the data in figure 7.5 along with a PSD cut set to exclude all but 10^{-4} of the gamms. The neutron band is not used for setting the PSD cut, but is used to determine the cut efficiency.

7.4 Time Distribution Fitting

With the exception of fusion neutrons which may be identified relatively easily, the most distinctive characteristic of the other signals is their time dependance. The time distributions of the signals overlap, so it is generally not possible to identify individual events with time cuts. However, by fitting the time distribution we can determine the number of events of

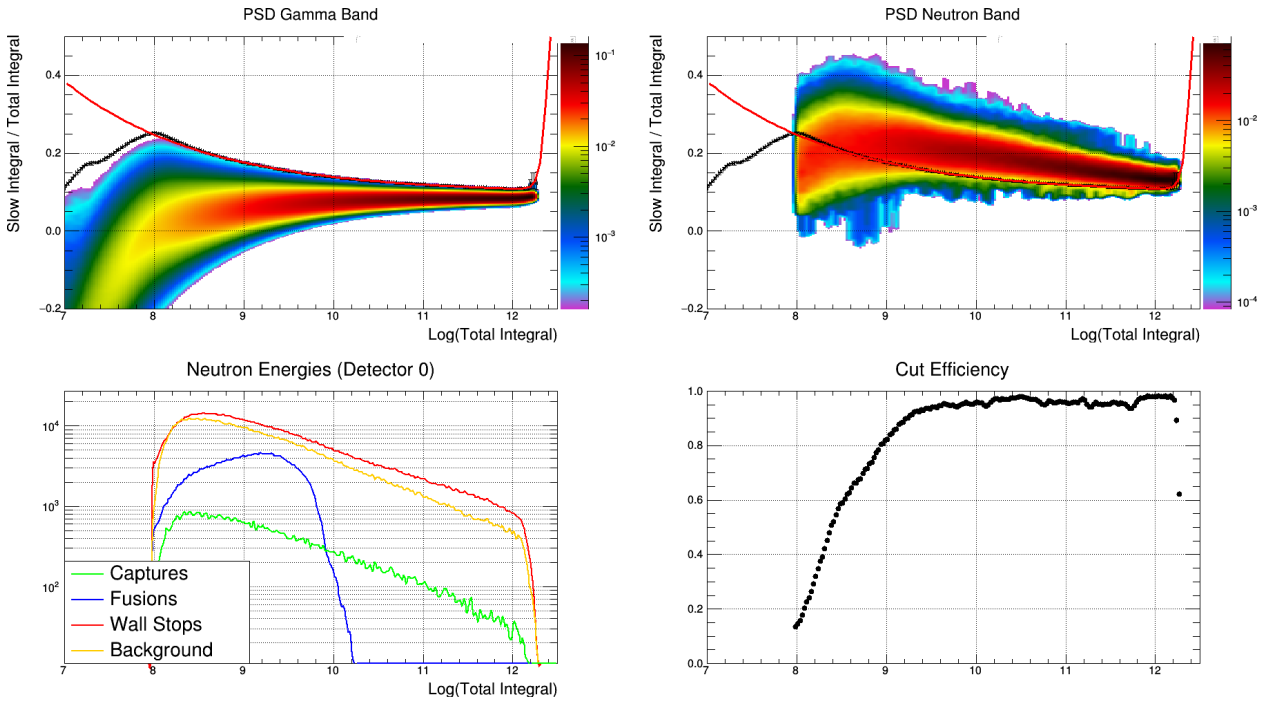

Figure 7.6: PSD plots of the estimated true gamma (left) and neutron bands (right)

each type. A fitting procedure designed to determine these signal components has been developed using RooFit.

7.4.1 Signal Shapes

A probability density function (PDF) is defined for each signal source. These PDFs are written as custom RooFit classes derived from a slightly modified PDF base class. The PDFs are designed for binned fits, and also respect variable binning schemes. This is necessary to capture the initial gamma pulse and wall stop signals with high resolution without sacrificing bin statistics in background-dominated regions. The PDFs also support software blinding by pre-scaling the time variable before it is passed to the fit function. This scaling mimics our hardware blinding of the master clock rate, and is equivilant to blinding all relevant rates by a certain fraction.

Exponentials

Most of the signal shapes should be either single or double exponentials starting after the muon entrance. The time alignment of the neutron detector and entrance signals is not completely precise, in the start time of the signals might have a slight offset from zero. This start time is not completely constant either, as downstream stops should be slightly more delayed and the time of flight to the detectors depends on the stop position and neutron energy. The variable times of flight for the incoming muon and outgoing neutrons, as well finite detector resolution, also causes the signals to become smeared out somewhat. Approximating this smearing by convolving the exponential signals with a gaussian kernel results in shapes known as exponentially modified gaussian functions.

The signals therefore have two unknown parameters: the width of the gaussian kernel and the time offset. These parameters are generally fit to the fiducial volume data, and then kept fixed for any subsequent fits. For gamma rays, the systematic shift in the start time due to the stop position is modeled with the equation

$$\Delta t = v_\mu r_\mu + c r_n \tag{7.7}$$

where v_μ is the muon speed of 1/3 c and r_μ and r_n are the distances from the stop position to the entrance window and neutron detector, respectively. This correction yields time offsets of at most $2ns$, but small shifts in the gamma ray start time are actually rather important. Because the atomic capture pulse coincides with the steep rising edge of the decay distribution, a small time offset can be mistaken an atomic capture signal and produce a false positive wall stop signal. The time offset due to the neutron time of flight is not currently modeled, but while it is larger than the gamma offset it is less critical without the atomic capture peak.

Atomic Capture Pulse

The atomic capture gammas produce a pulse that is only about $10ns$ long. Some of this width comes from the same smearing discussed for the exponential signals, but the pulse

also has some width of its own. In fact, the pulse should have a complicated structure since it originates from several atomic transitions occuring in turn with delays in between. This level of detail is not needed for such a short pulse though, and an adequate approximation is obtained by using a square pulse once again convolved with a gaussian kernel.

This pulse has three unknown parameters: the original time and width of the square pulse and the width of the gaussian kernel. Selecting stop distributions near either the anode or cathode results in a very prominent atomic capture peak that can be used to calibrate these fit parameters.

Background

The background signal shape will only be described briefly here, for a detailed description of the general background model see appendix A. The beam has separate kicked and un-kicked configurations which may have different average background rates and accelerator RF amplitudes. These four components may each have different energy spectra as well, causing the background shape to vary with energy. Immediately after the muon entrance, the beam must be in the un-kicked state. The kicker then fires and the beam stays in the kicked state until the end of the event window 25 μs later. Before the muon entrance the beam background is an admixture of the kicked and un-kicked states, depending on the probability of the previous kick being active at that point.

Some of the beam background parameters may be extracted from the muon entrance autocorrelation, such as the beam rate and the kick start and stop times. However, the kick times are offset for the backgrounds because they are partially determined by the time of flight from the kicker to the target. For secondary particles like the neutrons and gammas, it is also necessary to determine the decay rate of their parent particle to fit the kick transition. Thus, each background component has seven unknown parameters: the kick time and decay rate as well as the amplitudes of the four background components and the RF oscillation phase.

The gamma background oscillation amplitudes are determined using a specialized oscil-

lation histogram. This histogram saves the time modulo the RF frequency separately for neutrons before the muon entrance and more than 10 μs after the entrance. The kicked oscillations are fit directly to the late time signal. The un-kicked oscillations are determined by fitting the early time signal and subtracting the expected amplitude from the kicked oscillations. An example fit is shown in figure 7.7. An identical histogram is generated for the neutron background, but no oscillations are apparent so the oscillation amplitude is fixed to zero.

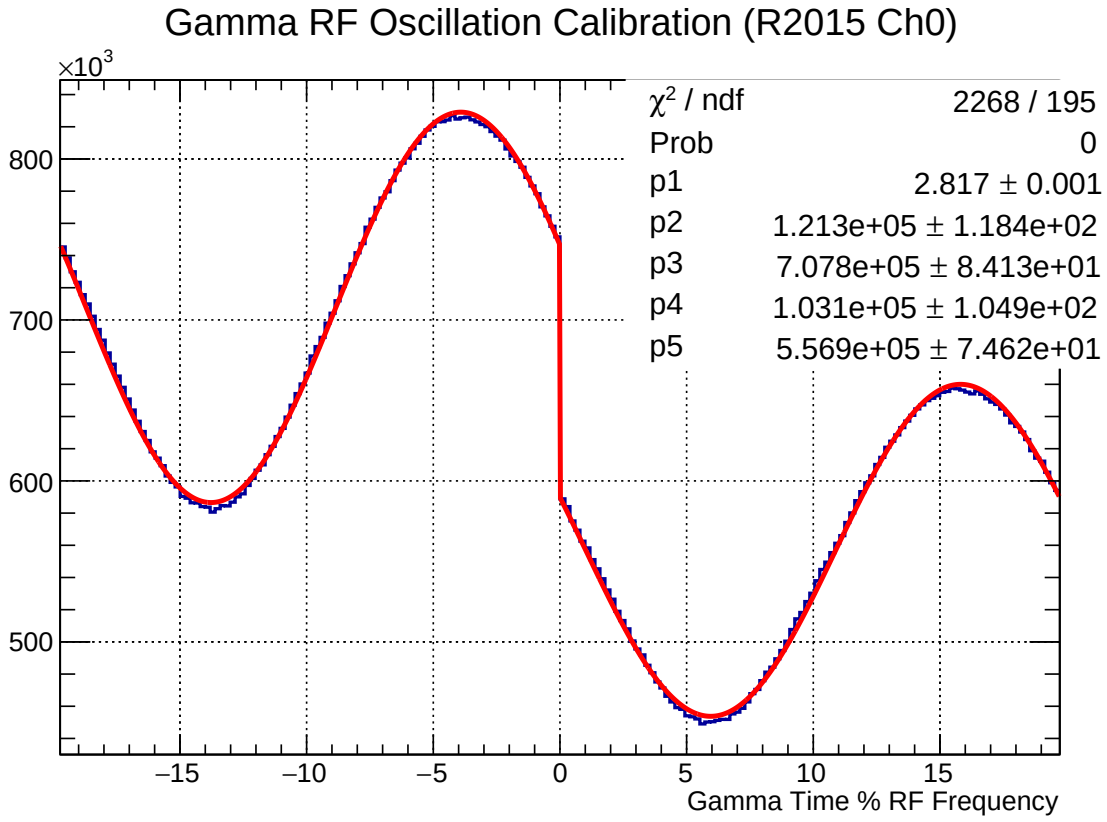

Figure 7.7: RF oscillation histogram with fit to sine waves with constant backgrounds. The χ^2 value is poor because the slopes of the background are not modeled, but the oscillation parameters should be reliable.

To study the kicker step in the neutron background, we can make a set of contradictory cuts to exclude all the real signals. The TPC energy cut is effective at eliminating fusions,

while a fiducial volume cut removes most wall stops and ensures no pulses are missed by the energy cut. An electron requirement cuts most capture events as well, and the electron coincidence veto cuts photo-neutrons. This leaves only normal decays with accidental neutrons, plus a small proportion of captures and photo-neutrons with accidental electrons. The gamma background can also be enhanced with similar cuts, but it is large enough that it can be studied more easily using the muon clock data.

7.4.2 Fit Procedure

The RooFit framework is very powerful and allows for a number of complicated fitting procedures such as multi-dimensional and simultaneous fits. For the neutron analysis we have 8 detector channels, each with neutron and gamma signals. A RooFit model is defined which simultaneously fits all 16 of these signals. Since many of the fit parameters are the same across detectors, this allows for significantly more precise results than individual fits.

The time dependence of the various signal components must agree between detectors, differing only by time offsets and possibly different time resolution. The signal strength observed in different detectors is also related, but it is more complicated. The way each signal varies across detectors depends on the source of the signal, which may be divided into three classes:

Beam Backgrounds

Beam background signals are the simplest to account for. These are uncorrelated with the observed muon stop by definition, so the properties of the muon are irrelevant. Beam backgrounds therefore scale directly with the number of muon stops selected. The relative background levels in each detector are usually set by an initial fit to the full statistics, and then are kept fixed in subsequent fits with various cuts applied. Currently the overall background level is allowed to float, but it could be fixed from the number of stops which would reduce the background fit to zero parameters.

Direct Signals

Signals produced directly by the muon include capture and fusion neutrons as well as atomic and nuclear capture gamma rays. These signals are also proportional to the number of muon stops, but unlike the beam backgrounds they are emitted at the muon stop position and radiate outwards. For stops that are off-center, this produces a larger observed signal in the closer detectors.

A solid angle correction is therefore applied to account for the distance to the detectors. This correction uses a 3D histogram of the stop distribution and calculates the solid angle coverage of each detector integrated over stop position. For each bin the events are treated as stopping uniformly across the bin volume. With the solid angle correction applied, these signals may also be reduced to a single amplitude parameter.

Scattering

Finally, the bremsstrahlung and photo-neutron signals originate from scattering in the TPC walls rather than directly from the muon. The signal strength therefore depends on the geometry of the detectors and support structure and becomes difficult to calculate. It may be possible to use Monte Carlo simulation data to estimate the detection efficiency as a function of stop position, but a data-driven approach would be better. For now, these signals must be fit to each channel individually.

7.5 Kinetics Calibration Results

7.5.1 Fusion Neutrons

7.5.2 Deuterium Capture

7.6 Wall Stop Results

7.6.1 Scans